Icarus 302 (2018) 418–425

Contents lists available at ScienceDirect

Icarus

journal homepage: www.elsevier.com/locate/icarus

Coloring Jupiter's clouds: Radiolysis of ammonium hydrosulfide (NH_4SH)

Mark J. Loeffler[a,b,*], Reggie L. Hudson[a]

[a] NASA Goddard Space Flight Center, Greenbelt, MD 20771, USA
[b] Northern Arizona University, Department of Physics and Astronomy, Flagstaff, AZ 86011, USA

ARTICLE INFO

Article history:
Received 12 June 2017
Revised 2 October 2017
Accepted 30 October 2017
Available online 10 November 2017

Keywords:
Jupiter, atmosphere
Ices, ultraviolet-visible spectroscopy
Geophysics
Atmospheres, chemistry
Experimental techniques

ABSTRACT

Here we present our recent studies on the color and spectral reflectance changes induced by ~0.9 MeV proton irradiation of ammonium hydrosulfide, NH_4SH, a compound predicted to be an important tropospheric cloud component of Jupiter and other giant planets. Ultraviolet-visible spectroscopy was used to observe and identify reaction products in the ice sample and digital photography was used to document the corresponding color changes at 10–160 K. Our experiments clearly show that the resulting color of the sample depends not only on the irradiation dose but also the irradiation temperature. Furthermore, unlike in our most recent studies of irradiation of NH_4SH at 120 K, which showed that higher irradiation doses caused the sample to appear green, the lower temperature studies now show that the sample becomes red after irradiation. However, comparison of these lower temperature spectra over the entire spectral range observed by HST shows that even though the color and spectrum resemble the color and spectrum of the GRS, there is still enough difference to suggest that another component may be needed to adequately fit spectra of the GRS and other red regions of Jupiter's clouds. Regardless, the presence of NH_4SH in the atmosphere of Jupiter and other gas giants, combined with this compound's clear alteration via radiolysis, suggests that its contribution to the ultraviolet-visible spectra of any of these object's clouds is significant.

1. Introduction

It is well-known that the optical properties of many solid materials can be modified by radiolysis and photolysis. For salts that are formed from the representative elements, radiation-induced modification can often be observed in the visible region, as the pristine material, which is typically white or colorless, will change color. These optical changes can be quantified using ultraviolet-visible (uv-vis) spectroscopy. For many salts, such as alkali halides (Schulman and Compton, 1962), such color changes are attributed to the formation of defect/color centers, which preferentially absorb visible light.

A salt that we have had an interest in over the last few years is ammonium hydrosulfide (NH_4SH). This salt is composed of NH_4^+ and HS^- ions, yet is somewhat unlike many other salts found on Earth in that under typical atmospheric conditions and room temperature it is unstable and promptly decomposes into H_2S and NH_3 gases. However, condensed NH_4SH is believed to be found in the clouds of many giant planets in our Solar System (e.g. Atreya et al., 1999; Sromovsky and Fry, 2010a,b; Roman et al., 2013), most notably Jupiter, where it is believed to be one of the main components found in the tropospheric clouds (Weidenschilling and Lewis, 1973).

The prediction of a significant presence of NH_4SH in the Jovian atmosphere is particularly interesting given that there are colored regions throughout the Jovian clouds. One of the most well-known regions is Jupiter's Great Red Spot (GRS). Interestingly, although the GRS may have been observed as early as the 1660s by Hooke and Cassini, the origin of its color is still unclear. Many candidates, including NH_4SH, have been suggested (West et al., 1986), with the most recent proposals coming from a residue produced by photolysis of a NH_3 and C_2H_2 gas mixture (Carlson et al., 2016; Sromovsky et al., 2017). One difficulty in correlating the color of the GRS or any other red region to a specific absorber is that such regions have no strong absorption bands in the uv-vis region, where most of the observational data is acquired. Thus, in this context "color" refers to the spectral slope below ~600 nm, which is steeper than the full-disk geometric albedo spectrum of Jupiter (Karkoschka, 1994). Furthermore, it has been shown that the GRS's color (i.e., spectral slope) varies with time being brown,

* Corresponding author at: Northern Arizona University, Department of Physics and Astronomy, 527 S. Beaver St, Bldg 19, Rm 209, Flagstaff, AZ 86011-6010, USA.
E-mail address: mark.loeffler@nau.edu (M.J. Loeffler).

https://doi.org/10.1016/j.icarus.2017.10.041
0019-1035/

red, beige, white, or even blue (Simon et al., 2015), indicating that the composition of the GRS may also be changing, potentially further complicating the discovery of a unique solution for the origin of the colors of Jovian clouds and the GRS.

Given that condensed NH_4SH is an important Jovian cloud component and that many salts change color via irradiation, it seems likely that this compound contributes to colors in Jupiter's atmosphere. However, there are few laboratory studies on NH_4SH to test this hypothesis. This is perhaps partly because NH_4SH must be synthesized in the laboratory, and that the most straightforward low-temperature synthesis involves two reactants, as shown in (1), that are toxic, odiferous, and somewhat detrimental to laboratory equipment.

$$NH_3(g) + H_2S(g) \rightarrow NH_4SH(s) \quad (1)$$

Over the past decade, we have made a concerted effort to study compounds that have astrochemical relevance, but that may have received little attention because of inherent difficulties associated with their preparation. Recent projects relevant to the Jovian system are the formation (Moore et al., 2007b), radiation stability (Loeffler et al., 2011), and thermal regeneration of sulfuric acid hydrates (Loeffler and Hudson, 2012), as well as the low-temperature thermally induced reactions between SO_2 and H_2O (Loeffler and Hudson, 2010), SO_2 and H_2O_2 (Loeffler and Hudson, 2013), H_2O_2 and NH_3 ices (Loeffler and Hudson, 2015), and O_3 and SO_2 ices (Loeffler and Hudson, 2016). In light of the problem concerning the GRS's color, we have recently begun studying the radiation chemistry of NH_4SH, using both IR (Loeffler et al., 2015) and uv-vis spectroscopy (Loeffler et al., 2016) as our main analytical tools. We are focusing on radiation chemistry because Jupiter's atmosphere is subject to energetic particle bombardment and solar-UV photolysis, which alter the chemical composition and perhaps color the originally featureless cloud components. Our studies showed that the sulfur reaction products possess broad absorption bands in the uv-vis spectra of NH_4SH (Loeffler et al., 2016), which were reasonably consistent with the only other laboratory work on NH_4SH chemistry (Lebofsky and Fegley, 1976). We also found in our previous studies that although irradiated NH_4SH shows a strong spectral feature that is absent from GRS spectra, causing our samples to appear green, warming such ices to temperatures still within the range of the atmospheric clouds removes this absorption, significantly improving the fit between the laboratory and remotely acquired spectra.

Given that our most recent paper only reported irradiations at one temperature, 120 K, and that heating our sample appears to change its composition, we decided to investigate how the radiation chemistry of NH_4SH changes with temperature. As in our previous studies, we use ~0.9 MeV protons as an analog to the low-energy, and more-abundant, cosmic rays present in the Jovian atmosphere. Specifically, we irradiated crystalline NH_4SH at 10–160 K with ~0.9 MeV protons, while monitoring the sample with uv-vis spectroscopy and digital imaging. These in situ measurements allow us to determine stability and chemical changes in our sample as a function of temperature and radiation dose and complement our previous IR studies over roughly the same temperature range. The results of such measurements reveal the role of irradiation temperature in altering chemical composition and whether any of the products formed from irradiated NH_4SH are plausible candidates for coloring the GRS or other regions in Jupiter's clouds.

2. Experimental

The experimental approach and NH_4SH preparation were as described in our first uv-vis study of NH_4SH (Loeffler et al., 2016), so only a brief summary is presented here. All experiments were performed in a high vacuum system (~1×10^{-7} torr) on a sand-blasted aluminum substrate, and all samples of solid NH_4SH were synthesized by depositing a mixture of H_2S and NH_3 at 90 K and warming it at 2 K min^{-1} to 160 K, where it was annealed for 30 minutes to ensure crystallization. We chose to focus on the crystalline phase of NH_4SH, because this is likely the starting phase of the ice at the temperature of the Jovian clouds (Loeffler et al., 2015), yet we point out that in this spectral region the initial phase of the ice did not appear to strongly affect our results. After crystallization, the samples were then cooled to the desired irradiation temperature. The thickness of all samples studied was ~17 μm.

We irradiated our NH_4SH ices with 0.924 MeV p+ (referred to in the text as ~0.9 MeV) which were of sufficient energy to pass through the entire ice sample; with the average energy loss being ~0.00035 eV μm^{-1} (Ziegler, 2010). Samples were biased at +35 V to minimize the loss of secondary electrons. The proton beam current typically was 100 nA, for an incident dose rate (flux) of about 1.3×10^{11} p+ cm^{-2} s^{-1} in NH_4SH.

Before, during, and after irradiation, spectra of ice samples were recorded at 250–1000 nm at a resolution of 1.5 nm using an Avantes ULS2048XL fiber optic spectrometer. Light was aimed directly at the sample's surface (0° incidence) and reflected light was collected at 9°. The small phase angle was chosen to make our results more directly comparable to Jovian observations. The reflectance of our samples is given by $R = (I_{sample} - I_{dark}) / (I_{reference} - I_{dark})$. In addition to measuring spectral reflectance, we also photographed our samples with a Canon Eos Rebel T3i camera. During the experiments the camera was mounted on a tripod and photographs were taken so that the field of view included both the sample and the surroundings to ensure that the lighting was consistent; the images were subsequently cropped to show only the sample. Preliminary experiments revealed that our uv source could alter an NH_4SH ice sample on the timescale of our experiments in a manner that was qualitatively similar to what we observed with low ion irradiation fluences. To minimize this problem, the light needed to collect reflectance spectra passed through a glass (BK-7) window, which decreased the intensity of uv light ($\lambda < 300$ nm) by an order of magnitude compared to a fused silica window. However, we also observed that the light source could alter the transmission properties of the window itself if left on for long periods of time, and thus we minimized the time our window was illuminated with the uv source and performed multiple checks to ensure that the observed spectral changes shown here were only due to changes in the ice sample. Future studies will investigate in more detail the effect of photolysis.

3. Results

3.1. Color formation

We irradiated crystalline NH_4SH at 10, 50, 120, and 160 K with ~0.9 MeV protons. Fig. 1 shows each sample after the same four radiation doses. Before irradiation, each sample was transparent and colorless, and thus only the gray aluminum substrate was evident. However, at low irradiation fluences (left columns), each sample developed a yellowish hue that was most evident at the lower irradiation temperatures. With increasing fluence, the yellowish hue evolved into a more reddish color at lower irradiation temperatures ($T < 50$ K), while at the higher irradiation temperatures it became green, rather than red.

We also irradiated NH_3 and H_2S ices at 50 K. These samples were grown so that they contained the same amount of nitrogen (or sulfur) atoms as the NH_4SH samples, i.e., they were about half as thick. Both NH_3 and H_2S were transparent and colorless before irradiation, and thus, like the NH_4SH ices, only the gray aluminum substrate is evident in photographs. Irradiation did not produce

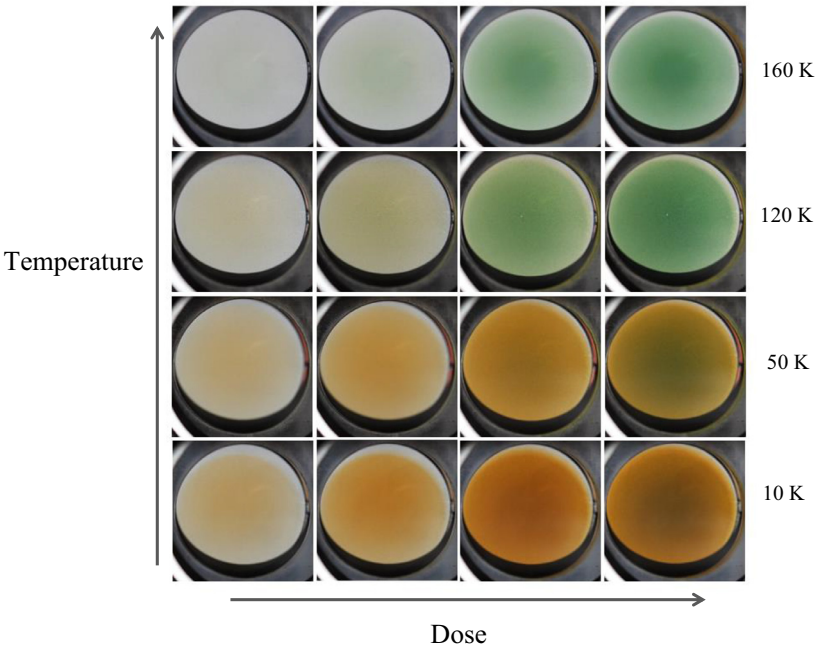

Fig. 1. Photographs of crystalline NH_4SH before and during irradiation at temperatures of 10, 50, 120 and 160 K with ~0.9 MeV protons. Each column corresponds to the following ion fluence (left to right): 0.08,: 0.31, 2.5, and 5.0×10^{13} p^+ cm^{-2}.

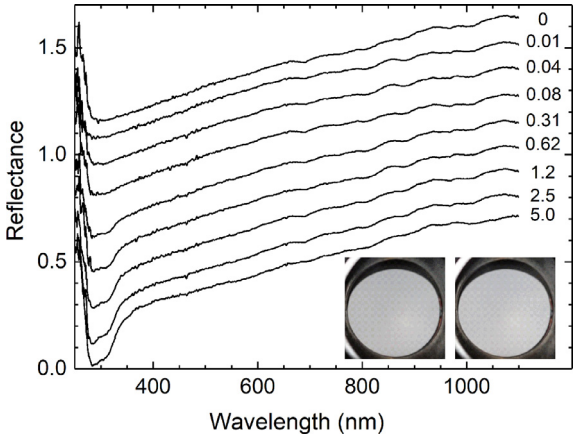

Fig. 2. Ultraviolet-visible spectra of crystalline NH_3 during irradiation at 50 K with ~0.9 MeV protons. The ion fluence is given at the right (in units of 10^{13} p+ cm^{-2}) of each spectrum. The spectra have been vertically offset for clarity. Photographs (from left to right) correspond to spectra taken after 0 and 5.0×10^{13} p+ cm^{-2}. The unshifted reflectance spectra have been included as supplementary data.

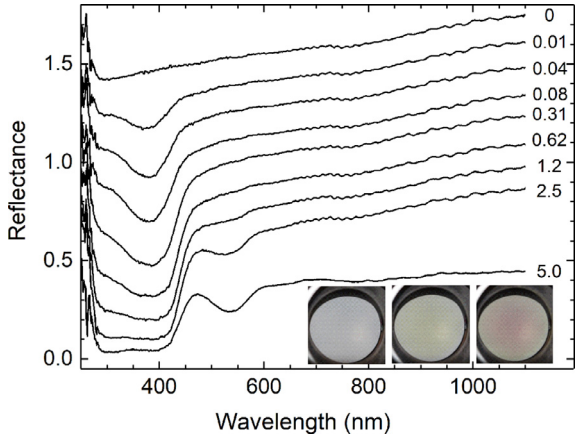

Fig. 3. Ultraviolet-visible spectra of crystalline H_2S during irradiation at 50 K with ~0.9 MeV protons. The ion fluence is given at the right (in units of 10^{13} p+ cm^{-2}) of each spectrum. The spectra have been vertically offset for clarity. Photographs (from left to right) correspond to spectra taken after 0, 0.62, and 5.0×10^{13} p+ cm^{-2}. The unshifted reflectance spectra have been included as supplementary data.

any colors in the NH_3 samples (see Fig. 2 inset), but it did cause the H_2S ice to change color (see Fig. 3 inset). In fact, the color change observed in H_2S was qualitatively similar, albeit fainter, to that in NH_4SH irradiated at 50 K: initially the ice developed a yellowish hue and at higher fluences became reddish.

3.2. UV-visible spectroscopy

In addition to photographing our irradiated samples, we also monitored them with uv-vis spectroscopy. The uv-vis spectrum of unirradiated crystalline NH_4SH is shown in the top of Fig. 4. Longer than 300 nm, the spectrum is essentially featureless and the reflectance increases slightly with wavelength. The decrease in reflectance below 300 nm is due to absorption by SH^-, which is centered near 230 nm (Ellis and Golding, 1959; Guenther et al., 2001). The remaining reflectance spectra in the top panel of Fig. 4 were taken after irradiation with ~0.9 MeV protons at 50 K. At low fluences an absorption band centered near 425 nm is clearly resolved. At higher fluences, the band becomes broader, particularly on the low wavelength side, and another band centered near 610 nm becomes evident as well. Changing the irradiation temperature did not alter the spectra drastically, although differences were observed (see 160 K irradiation in middle panel of Fig. 4). For instance, the 610 nm absorption was seen at lower fluences and was better resolved at 160 K than at 50 K (see Fig. 4).

We also compared our NH_4SH spectral results with those from reference (blank) experiments in which NH_3 and H_2S ices and the bare aluminum substrate were irradiated at 50 K. As expected, the bare substrate showed no change within the error of our measurements (<1%). The evolution of the ultraviolet-visible reflectance spectra of our NH_3 and H_2S ices during irradiation at 50 K is shown in Figs. 2 and 3, respectively. Longer than ~350 nm, the NH_3 spec-

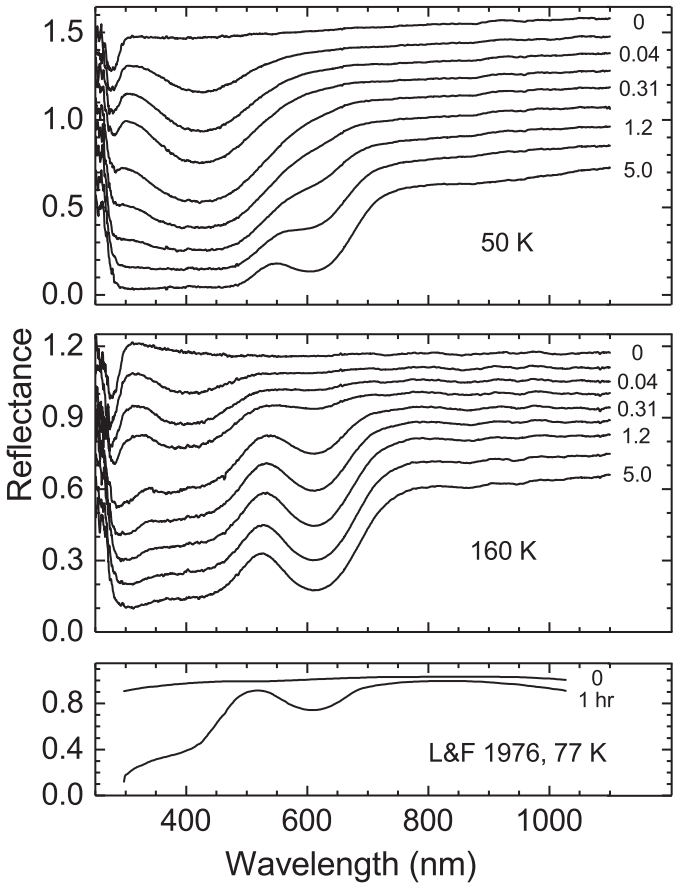

Fig. 4. Top and middle panels: ultraviolet-visible spectra of crystalline NH_4SH during irradiation at 50 K and 160 K with ~0.9 MeV protons. From top to bottom in each panel, the ion fluence (in units of 10^{13} p+ cm^{-2}) for each spectrum is: 0, 0.01, 0.04, 0.08, 0.31, 0.62, 1.2, 2.5, and 5.0. The spectra have been vertically offset for clarity. The unshifted reflectance spectra from our experiments have been included as supplementary data. Corresponding photographs are shown in Fig. 1. Bottom panel: ultraviolet-visible spectra of NH_4SH before and after 1 h of photolysis at 77 K (data extrapolated from Lebofsky and Fegley, 1976).

trum remained virtually unchanged, consistent with previous studies (Lebofsky and Fegley, 1976). However, an absorption around 300 nm formed at higher fluences during the NH_3 irradiation. In contrast to the NH_3 data, the H_2S spectra changed during irradiation in a manner qualitatively similar to the irradiated NH_4SH ice, although the peak positions were slightly shifted. For instance, at low fluences a band near 380 nm formed. Continued irradiation caused this band to broaden on the low wavelength side, as in the case of NH_4SH. At higher fluences, a new band near 535 nm formed in the irradiated H_2S ice, similar to what was seen at 610 nm for NH_4SH.

4. Discussion

4.1. Radiation chemistry

One characteristic of ammonium hydrosulfide that makes its radiation chemistry interesting is that this solid is not composed of NH_4SH molecules, but rather of ammonium (NH_4^+) and bisulfide (SH^-) ions. Thus, the chemical changes induced by radiolysis are complex, as the products may not only form from each of these individual ions but also from a combination of the two. The only publications on the reaction chemistry of NH_4SH are the radiation-chemical studies from our laboratory (Loeffler et al., 2015, 2016) and an earlier paper on the photochemistry of NH_4SH (Lebofsky and Fegley, 1976). The later work and our most recent publication (Loeffler et al., 2016) were restricted to one temperature, with uv-vis reflectance spectroscopy as the main analytical technique, whereas our initial study (Loeffler et al., 2015), used IR spectroscopy as the main analytical tool and covered 10–160 K. The following discussion is based on those previous studies.

Exposure of solid ammonium hydrosulfide to ionizing radiation, such as our p+ beam, produces tracks of ionizations and excitations through the sample from the thousands of secondary electrons generated by each incident proton. The expected initial reaction steps for NH_4^+ are

$$NH_4^+ \rightarrow NH_4^{+*} \rightarrow NH_3^+ + H \quad (2)$$

$$NH_4^+ \rightarrow NH_4^{+*} \rightarrow NH_4^{2+} + e^- \quad (3)$$

The NH_3^+ is expected to remain in our ices to temperatures as high as 170 K (Cole, 1961; Hyde and Freeman, 1961), while the NH_4^{2+} shown in (3) should react with the anion, SH^- (a strong base) to form H_2S

$$NH_4^{2+} + SH^- \rightarrow NH_3^+ + H_2S \quad (4)$$

In addition to (2) or (3), the excited ammonium ion could also react with SH^- to form H_2S. Combination of NH_3^+ and e^- will regenerate NH_3. Alternatively, if an adjacent ion pair is excited, then NH_3 and H_2S will be produced. If NH_3 and H_2S are produced in close proximity, then they should react to reform the original cation and anions in the sample.

For SH^-, we expect reactions similar to those described for NH_4^+ involving ionization

$$SH^- \rightarrow SH^{-*} \rightarrow S^{2-} + H^{+} \quad (5)$$

$$SH^- \rightarrow SH^{-*} \rightarrow S + H + e^- \quad (6)$$

$$SH^- \rightarrow SH^{-*} \rightarrow SH + e^- \quad (7)$$

The mercapto (SH) radical in (7) has been reported as one of the main products formed in low-temperature photolysis of H_2S (Stiles et al., 1966). The sulfur atoms in (6) can react, resulting in longer-chained species, such as:

$$S + SH^- \rightarrow HS_2^- \quad (8)$$

$$\rightarrow H^+ + S_2^{2-} \quad (9)$$

The 425 nm band seen in our spectra is likely caused by the sulfur products in (8) and (9), which have also been observed in liquid solutions (Giggenbach, 1972). Either of the anions formed in (8) or (9) could also produce the $S_3^{-\bullet}$ radical we observed at 610 nm (Holzer et al., 1969; Chivers and Drummond, 1973; Chivers and Lau, 1982; Dubois et al., 1987) through a reaction with the SH radical produced in (7):

$$SH + HS_2^- \rightarrow S_3^{-\bullet} + H_2 \quad (10)$$

Buildup of a significant amount of $S_3^{-\bullet}$ can cause dimerization, forming S_6^{2-} through

$$2\ S_3^{-\bullet} \rightarrow S_6^{2-} \quad (11)$$

which also likely contributes to this broad shorter wavelength absorption, given that S_6^{2-} has been observed between 410 and

Table 1
Summary of absorption band positions, colors, and identifications in our ices after ion irradiation.

Absorption bands				
	Irradiated NH_4SH		**Irradiated H_2S**	**Irradiated NH_3**
λ (nm)	425	610	375	300
Assignment	HS_2^-, S_2^{2-}, S_3N^-, $S_2^{-\bullet}$	$S_3^{-\bullet}$	S_n, H_2S_x	N_3^-

Sample color			
	Irradiated NH_4SH	**Irradiated H_2S**	**Irradiated NH_3**
All T, low doses	Yellow	Pale yellow	None
50 K, high doses	Red	Pale red	None
120 K, high doses	Green	–	–

480 nm in solution (Dubois et al., 1988, 1989; Prestel and Schindewolf, 1987). Other key contributors to this shorter wavelength region could be neutral amorphous sulfur (Dubois et al., 1988), which would result from a build-up of sulfur atoms in the ice.

Besides chemical reactions that form primarily N-bearing or S-bearing products, we also expect products that contain both of these atoms. The one product that is consistent with our spectra and previous IR studies (Loeffler et al., 2015) is the S_xN^- anion. A possible pathway to form S_xN^- would involve radiolytically produced NH_3 and a large number of sulfur atoms. A likely candidate, given the published IR (Bojes et al., 1982), Raman (Chivers and Lau, 1982), and UV absorptions is S_3N^- (Chivers and Lau, 1982), which shows absorptions at 666 cm^{-1}(15.015 μm), 686 cm^{-1}(14.577 μm) and 425 nm, respectively. A possible formation pathway would resemble that given by Dubois et al. (1987):

$$9\ S + 3\ NH_3 \rightarrow S_3N^- + 2\ S_3^{-\bullet} + 3\ NH_4^+ \quad (12)$$

4.2. Sample color

The reflectance spectrum of unirradiated NH_4SH only changed by 4% across the visible spectral region (390–700 nm), making it colorless to the eye. However, irradiation quickly caused the sample to change color, producing various shades of red, yellow, or green, which depended on both the ion fluence and the irradiation temperature (see Table 1 for summary). The first spectral band, likely from HS_2^-, S_2^{2-}, or S_3N^-, is at 425 nm, at the edge of the visible region and causing the sample to appear yellow. Other contributors to the yellow color could be $S_2^{-\bullet}$, which may precede the formation of $S_3^{-\bullet}$, or the dimer, S_6^{2-} (Chivers and Drummond, 1973; Raulin et al., 2011). Further irradiation broadened this band, causing the yellow wavelengths to become absorbing, leaving the red wavelength as the most reflective. At low irradiation temperatures, this reddish color dominated, yet at the higher irradiation temperature the $S_3^{-\bullet}$ radical's absorption band near 610 nm, which by itself would cause the sample to appear blue (Chivers and Elder, 2013), was more pronounced. This absorption covered the longer wavelength region that preferentially absorbed red light, resulting in giving the sample a greenish hue.

4.3. Comparison with previous work

Besides our recent work (Loeffler et al., 2016), the only other published study of NH_4SH over our wavelength range is the UV photolysis work of Lebofsky and Fegley (1976), which we show for comparison in the bottom panel of Fig. 4. Our uv-vis spectra before proton irradiation in Fig. 4 (top), which show that the sample lacks absorption features over the visible region, are consistent with Lebofsky and Fegley (1976). In addition, the position and general shape of the absorption features observed in our NH_4SH ice's spectra after proton irradiation are also in agreement with those observed after photolysis (see Fig. 4 bottom). The similarity of the two spectra after the ice has been modified by UV photons or MeV protons, suggesting the formation of similar products, is consistent with what we have observed previously for other ices (e.g., Gerakines et al., 2000; Hudson and Moore, 2001) and is evidence that most of the chemical changes result from the secondary electrons being formed during ion irradiation and UV photolysis.

Although the new products appear to be similar in the two experiments, the different assignments given by each study merit comment. Lebofsky and Fegley (1976) attributed absorptions below 500 nm to ammonium polysulfides, $(NH_4)_2S_x$, where x = 5–7, but since NH_4^+ does not absorb there, the actual chromophore must be one or more polysulfur anions (S_5^{2-}–S_7^{2-}). This is consistent with our and previous identifications, although we suggest that the polysulfur anion could also be a shorter chain (e.g., x = 1) as well. We also point out that S_xN^- ions, such as S_3N^-, will also contribute to absorption below 500 nm. Saying more to definitively identify the exact sulfur anion that is formed using absorptions in this region would be difficult, as spectral overlap is considerable. Besides the shorter wavelength absorption observed, both studies also clearly showed an absorption near 600 nm. Lebofsky and Fegley (1976) used Extended Hückel calculations to suggest S_x radical (x = 5–7) as the source. While our post-irradiation heating results (Loeffler et al., 2016) are consistent with this absorption being from a radical, we think $S_3^{-\bullet}$ is a more likely candidate, which is consistent with previous Raman (Holzer et al., 1969), uv-vis (Holzer et al., 1969; Chivers and Lau, 1982), and IR studies (Holzer et al., 1969; Loeffler et al., 2015).

The other ices irradiated, NH_3 and H_2S, also merit a few comments. Spectra of ion irradiated H_2S in our work and UV photolyzed H_2S in Lebofsky and Fegley (1976) are similar, and also resemble spectra of irradiated NH_4SH. In each case they have a single absorption near 600 nm and decrease in reflectance below ~500 nm. These similarities support the idea that the main observable products formed during UV photolysis and ion irradiation are predominately sulfur-bearing ions and molecules. However, spectra of our proton-irradiated H_2S ices differ from those of both the NH_4SH ices and the photolyzed H_2S ices in that the characteristic absorptions appear to be shifted to shorter wavelengths, with higher wavelength absorption appearing near 535 nm and the decrease in the UV beginning between 425 and 475 nm (depending on irradiation dose). Given the similarity of the photolyzed and radiolyzed ices in NH_4SH experiments, it is unclear why there is this difference for H_2S ices. Regardless, we can make spectral assignments in our experiments based on previous studies. The 535-nm absorption is likely due to longer-chained sulfur molecules, in particular S_4, which has been observed to absorb at ~530 nm in low-temperature (20 K) inert gas matrices (Meyer et al., 1972). Similarly, other molecules of the form S_n strongly absorb in this region (Eckert and Steudel, 2003) and likely contribute to the shorter wavelength absorption as well, even if their concentration is low. Finally, previous IR studies have shown that one of the main products resulting from irradiation of H_2S-ices is of the form H_2S_x (Moore et al., 2007b; Strazzulla et al., 2009; Loeffler et al., 2015), where $x \geq 2$, making it also a likely contributor to the shorter wavelength absorption. For NH_3-ice, UV photolysis induces a nominal change in the reflectance spectrum, whereas we observe an absorption near 300 nm at high doses in our experiments. This difference is likely because the absorptivity of solid NH_3 is very low (Dawes et al., 2007) at the range of wavelengths emitted by the xenon lamp (220–300 nm) used by Lebofsky and Fegley (1976). From the expected products of NH_3, the most likely candidate is N_3^- (Delcourt et al., 1976; Moore et al., 2007a, Parent et al., 2009), although it absorbs at a slightly higher wavelength than expected from liquid studies.

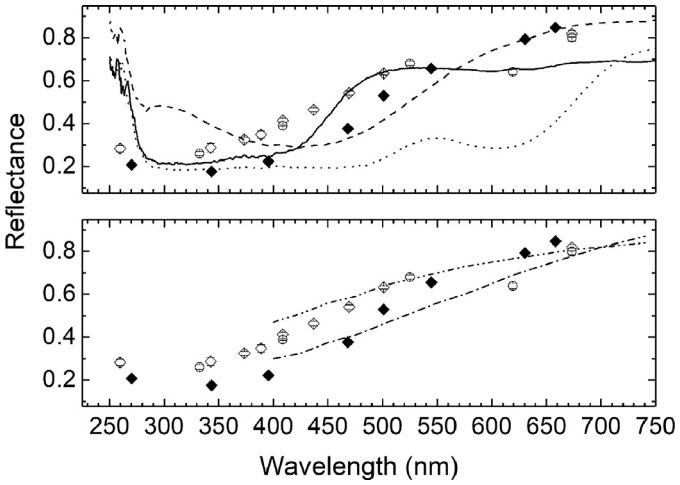

Fig. 5. Top: Comparison of the ultraviolet-visible spectra of irradiated crystalline NH_4SH with HST observations of the GRS from 1995 (o), 2008 (◊), and 2015 (♦). The laboratory spectra of NH_4SH are after the sample was irradiated at 50 K to a dose of 3×10^{12} ions cm^{-2} (dashed line) then 5×10^{13} p+ cm^{-2} (dotted line). Also included is the NH_4SH sample irradiated at 120 K to a dose of 5×10^{13} p+ cm^{-2} and warmed to 200 K (solid line; Loeffler et al., 2016). The laboratory spectra are vertically offset to match the GRS observational data. Bottom: Comparison of the spectra from Carlson et al. (2016) with the HST data. The laboratory spectra were derived from experiments that photolyzed NH_3+C_2H_2 at room temperature ($\delta R/R$ = 1/100, dash-dot-dot line; $\delta R/R$ = 16/100, dash-dot line). Error bars given for the HST data shown in both panels have been described previously (Loeffler et al., 2016); the error in the 2015 HST data is shown but is smaller than the symbol.

4.4. Giant-planet considerations

A robust quantitative comparison of our laboratory data to atmospheric spectra, which depend on a number of parameters in addition to composition (Strycker et al., 2011), would require derivation of optical constants of our irradiated ice sample. However, the similarity between the viewing geometry used to observe the GRS as well as other red regions of Jupiter and our experimental configuration still lends itself well for a qualitative comparison. Although the uv-vis region is difficult for diagnostic purposes, we see that the spectrum of the GRS is characterized by having high reflectance at the longer wavelengths, a strong slope at intermediate wavelengths, and being relatively flat at the shorter wavelengths (Fig. 5). In the data presented here, the best fit and corresponding best color is that of the low-temperature spectrum at low doses (Fig. 5 top). However, one can see that these data seem to diverge below 400 nm. Higher dose irradiations improve the fit at shorter wavelengths, but the appearance of $S_3^{-\bullet}$ lessens the quality of the fits in the region responsible for the color. A similar comment can be made about the sample irradiated at the higher temperatures (see Fig. 4 middle panel), yet the discrepancy at longer wavelengths is more drastic. Regardless, even though the visible appearance of our sample (red color) at low temperatures has the reddish color routinely ascribed to the GRS, it is clear that none of these irradiation temperatures can completely reproduce the entire spectrum of the GRS, underscoring the importance of using the largest spectral range for comparison as possible. We note that we have previously reported (Loeffler et al., 2016) that warming any of these samples to 200 K causes the long wavelength absorption to disappear, improving the spectral fit significantly (see Fig. 5 top). Thus, upon considering both our old and new data, the spectrum of annealed irradiated NH_4SH still gives the best fit to the spectrum of the GRS.

The only other recent laboratory work on the problem of Jovian colors comes from Carlson et al. (2016), who photolyzed a NH_3 + C_2H_2 gas-phase mixture and recorded the visible spectrum of the resulting solid residue. The data were used in a theoretical model of reflectance spectra of NH_3 grains with a coating of the same photolytic residue, and a reasonable fit was obtained to the GRS's spectral slope at 400–740 nm, which is shown in Fig. 5 (bottom), along with the data from HST. The fit to the HST data is comparable to our low dose data over this spectral range, and thus it would be interesting to know how the spectrum of the Carlson et al. (2016) photolyzed mixture changes below 400 nm, as the potential for a contributor other than one of the main cloud components is an interesting possibility. The need for more data points at not only the shorter wavelengths but also longer ones is evidenced by this group's most recent work (Sromovsky et al., 2017), where the Carlson et al. (2016) laboratory data (400 nm–740 nm) was linearly extrapolated so that it extended from 350 to 1060 nm. This data yielded adequate fits to multiple regions in Jupiter's clouds, yet it is important to note that the validity of such a linear extrapolation is unknown and can only be tested via laboratory measurements.

In addition, we also point out even with a larger spectral range, it is unclear if the trace amounts of C_2H_2 in Jupiter's upper atmosphere (Moses et al., 2010) could produce any of the spectral changes seen in the Carlson et al. (2016) laboratory experiments. For instance, at the altitude where the NH_3 and C_2H_2 ratio is similar to what was used in those experiments, the molar fraction of these species is only $\sim 10^{-10}$ (Moses et al., 2010). In addition, the laboratory reactions and measurements of Carlson et al. (2016) were conducted at room temperature (~295 K), not the much lower temperatures of Jupiter's upper atmosphere, and the uv source used was not a solar simulator but rather a lamp with three wavelengths, all at 202–214 nm. Future gas-phase studies with conditions more aligned with those of the Jovian atmosphere, such as lower temperatures, a lower C_2H_2 abundance, the presence of H_2 and He, and over a slightly larger wavelength range could further elucidate the applicability of such photolysis experiments to the GRS's color.

4.5. Timescales and temperatures

An important measure of the applicability of the laboratory data to the planetary environment is whether the radiation doses used in experiments are achievable on timescales relevant to the Jovian clouds. For the case of the GRS, we have made this estimate recently (Loeffler and Hudson, 2016) but give a brief summary here. Using the cosmic-ray energy flux of 9×10^{-3} ergs cm^{-2} s^{-1} of given by Sagan and Thompson (1984), a dose of $\sim 10^{13}$ ions cm^{-2}, which is approximately between the two lab spectra shown in Fig. 5, would correspond to about 30 years of cosmic ray exposure. This is likely an upper limit for the time needed for chemical alteration of the GRS, as this feature extends to higher altitudes than other cloud features (Simon-Miller et al., 2002), which may allow other, less penetrating, forms of radiation to modify the NH_4SH grains. To determine whether this time is comparable to the time during which the GRS is going to be chemically altered is not trivial, but since models suggest material arising in the center of Jupiter's Oval BA should thoroughly mix throughout the entire vortex on a timescale somewhere between months (de Pater et al., 2010) or decades (Conrath et al., 1981), we can at least say that our timescales appear reasonable. Of course we point out that the actual exposure time of an NH_4SH grain could be much shorter, as the signature of NH_3 grains detected in Jupiter's atmosphere was lost ~ 40 h after they first appeared (Reuter et al., 2007). However, it is possible that another material may have simply coated the grains (Atreya et al., 2005; Reuter et al., 2007); a thin coating

of this nature will not impede cosmic ray ions from altering the underlying grain material.

The temperatures used in our experiments also merit comment. In our experimental setup, NH_4SH is not thermally stable at temperatures above ~160 K, so we only performed irradiations up to 160 K. While these temperature are lower than the predicted temperature of a pristine NH_4SH cloud layer (~200 K), assuming a pressure of 1–2 bar (Wong et al., 2015), they are directly comparable to the temperature of the GRS, which ranges between ~110 and 130 K, depending on the location within the cloud (Simon-Miller et al., 2002; Fletcher et al., 2010). Thus, if the GRS can upwell gas from below (Carlson et al., 2016), then NH_4SH would be exposed to cosmic rays at the temperatures studied in our experiments. As we have noted previously (Loeffler et al., 2016), if radiolysis of NH_4SH mainly occurs at the 1–2 bar level near 200 K, we suspect that the spectral characteristics of the irradiated cloud will be similar to our samples that were irradiated at 120 K and 160 K but then warmed to 200 K, as both appear similar once they have reached 200 K. Finally, even though the colder irradiation temperatures we studied were mainly motivated by the desire to determine whether the radiation effects changed significantly with temperature, they may have some relevance to other giant planets, where temperatures in the upper atmosphere can be much lower. However, as equilibrium cloud models suggest NH_4SH will form at temperatures similar to those predicted for Jupiter (Atreya and Wong, 2005), a process, such as upwelling, would still be needed to bring NH_4SH high enough in the atmosphere to experience these lower temperatures.

5. Conclusions

We have irradiated crystalline ammonium hydrosulfide, NH_4SH, at 10–160 K with ~0.9 MeV protons, while monitoring the sample with uv-vis spectroscopy and photography. We found that irradiation causes the initially transparent and colorless sample to acquire a color that depends strongly on both the irradiation dose and temperature. At low doses, all samples turned yellow, while at higher doses we observed that a sample irradiated at a low temperature turned red, while a sample irradiated at a higher temperature turned green. The difference between the red and green samples is due to the greater prominence of the $S_3^{-\bullet}$ radical in the high temperature irradiation, which preferentially absorbs the red color, leaving the sample green. We also irradiated NH_3 and H_2S ices at 50 K for comparison with our NH_4SH ices. The general shape of the spectrum of irradiated H_2S is similar to that of NH_4SH ice, yet the absorption positions are slightly different. The difference between these two ices is attributed to the different radiation products formed, as the likely products in the H_2S-ice are molecules, while the products in the NH_4SH-ice are sulfur anions due to acid-base shifts.

In terms of the role that irradiated NH_4SH may play in coloring the GRS, we find that the spectral slope of our ice irradiated at low doses and at low temperatures is a reasonable match to what has been observed in GRS spectra longer than 400 nm, yet there is deviation between 300 and 400 nm. Higher dose irradiations show a nice fit at the shorter wavelengths, but the appearance of the $S_3^{-\bullet}$ band at higher wavelengths does not agree with what is observed in the HST spectra. After comparison with this new low temperature data, it seems evident that the best fit of a single NH_4SH ice is one that has been irradiated and warmed up to higher temperatures, so as to remove the $S_3^{-\bullet}$ radical that absorbs at 610 nm. Now that we have studied the radiolysis of NH_4SH over a range of doses and temperatures for both the uv-vis and infrared regions, we plan on future studies focusing on including other compounds that could also contribute to the spectrum of the GRS and other red regions of Jupiter.

Acknowledgments

The support of NASA's Planetary Atmospheres and Outer Planets Research programs is gratefully acknowledged. Steve Brown, Tom Ward, and Eugene Gerashchenko, members of the NASA Goddard Radiation Effects Facility, operated and maintained the Van de Graaff accelerator. This work used NASA/ESA Hubble Space Telescope observations retrieved from the Data Archive at the Space Telescope Science Institute, which is operated by the Association of Universities for Research in Astronomy, Inc. under NASA contract NAS 5-26555. The observations are associated with programs GO5313, GO11498, and GO13937, and using these program numbers all data can be retrieved from http://archive.stsci.edu/hst/search.php at the Hubble archive.

Supplementary materials

Supplementary material associated with this article can be found, in the online version, at doi:10.1016/j.icarus.2017.10.041.

References

Atreya, S.K., Wong, A.S., 2005. Coupled clouds and chemistry of the giant planets - a case for multiprobes. Space Sci. Rev. 116, 121–136.
Atreya, S.K., et al., 2005. Jupiter's ammonia clouds—localized or ubiquitous? Plan. Spac. Sci. 53, 498–507.
Atreya, S.K., et al., 1999. A comparison of the atmospheres of Jupiter and Saturn: deep atmospheric composition, cloud structure, vertical mixing, and origin. Plan. Spac. Sci. 47, 1243–1262.
Bojes, J., et al., 1982. The thio analogue of Peroxynitrite, [SSNS]-: Preparation, electronic structure, resonance raman spectrum, and formation of complexes with nickel and cobalt. J. Amer. Chem. Soc. 104, 4837–4841.
Carlson, R.W., et al., 2016. Chromophores from photolyzed ammonia reacting with acetylene: application to Jupiter's Great Red Spot. Icarus 274, 106–115.
Chivers, T., Drummond, I., 1973. The chemistry of homonuclear sulphur species. Chem. Soc. Rev. 2, 233–248.
Chivers, T., Elder, P.J.W., 2013. Ubiquitous trisulfur radical anion: fundamental and applications in materials science, electrochemistry, analytical chemistry, and geochemistry. Chem. Soc. Rev. 42, 5996–6005.
Chivers, T., Lau, C., 1982. Raman spectroscopic identification of the S_4N^- and S_3^- ions in blue solutions of sulfur in liquid ammonia. Inorg. Chem. 21, 453–455.
Cole, T., 1961. Paramagnetic defects in irradiated NH_4ClO_4. J. Chem. Phys. 35, 1169–1173.
Conrath, B.J., et al., 1981. Thermal structure and dynamics of the Jovian atmosphere. II - Visible cloud features. J. Geophys. Res. 86, 8769–8775.
Dawes, A., et al., 2007. Morphological study into the temperature dependence of solid ammonia under astrochemical conditions using vacuum ultraviolet and Fourier-transform infrared spectroscopy. J. Chem. Phys. 126, 244711.
de Pater, I., et al., 2010. Persistent rings in and around Jupiter's anticyclones – Observations and theory. Icarus 210, 742–762.
Delcourt, M.O., et al., 1976. Spectrophotometric studies of radiolysis of liquid-ammonia. J. Phys. Chem. 80, 1101–1105.
Dubois, P., et al., 1987. Chemical species in solutions of sulfur in liquid ammonia. Inorg. Chem. 26, 1897–1902.
Dubois, P., et al., 1988. Chemical-species in sulfur ammonia solutions - influence of amide addition. Inorg. Chem. 27, 3032–3038.
Dubois, P., et al., 1989. Photochemical observations in solutions of sulfur in liquid ammonia. Inorg. Chem. 28, 2489–2491.
Eckert, B., Steudel, R., 2003. Molecular spectra of sulfur molecules and solid sulfur allotropes. Elemental Sulfur und Sulfur-Rich Compounds II. R. Steudel. Springer, Berlin Heidelberg, pp. 31–98.
Ellis, A.J., Golding, R.M., 1959. Spectrophotometric determination of the acid dissociation constants of hydrogen sulfide. J. Chem. Soc. 0, 127–130.
Fletcher, L.N., et al., 2010. Thermal structure and composition of Jupiter's Great Red Spot from high-resolution thermal imaging. Icarus 208, 306–328.
Gerakines, P.A., et al., 2000. Carbonic acid production in H_2O:CO_2 ices. UV photolysis vs. proton bombardment. A&A 357, 793–800.
Giggenbach, W., 1972. Optical-spectra and equilibrium distribution of polysulfide ions in aqueous-solution at 20 degrees. Inorg. Chem. 11, 1201–1207.
Guenther, E.A., et al., 2001. Direct ultraviolet spectrophotometric determination of total sulfide and iodide in natural waters. Anal. Chem. 73, 3481–3487.
Holzer, W., et al., 1969. Raman spectra of negative molecular ions doped in alkali halide crystals. J. Mol. Spec. 32, 13–23.
Hudson, R.L., Moore, M.H., 2001. Radiation chemical alterations in solar system ices: an overview. J. Geophys. Res. 106, 33275–33284.
Hyde, J.S., Freeman, E.S., 1961. E.P.R. observation of NH_3^+ formed by x-ray irradition of ammonium perchlorate crystals. J. Phys. Chem. 65, 1636–1638.
Karkoschka, E., 1994. Spectrophotometry of the Jovian planets and Titan at 300- to 1000-nm wavelength: the methane spectrum. Icarus 111, 174–192.

Lebofsky, L.A., Fegley, M.B., 1976. Laboratory reflection spectra for determination of chemical composition of icy bodies. Icarus 28, 379–387.
Loeffler, M.J., Hudson, R.L., 2010. Thermally-induced chemistry and the Jovian icy satellites: a laboratory study of the formation of sulfur oxyanions. Geophys. Res. Lett. 37, 19201.
Loeffler, M.J., Hudson, R.L., 2012. Thermal regeneration of sulfuric acid hydrates after irradiation. Icarus 219, 561–566.
Loeffler, M.J., Hudson, R.L., 2013. Low-temperature thermal reactions between SO_2 and H_2O_2 and their relevance to the Jovian icy satellites. Icarus 224, 257–259.
Loeffler, M.J., Hudson, R.L., 2015. Descent without modification? The thermal chemistry of H_2O_2 on Europa and other icy worlds. Astrobiology 15, 453–461.
Loeffler, M.J., Hudson, R.L., 2016. What is eating ozone? Thermal reactions between SO_2 and O_3: implications for icy environments. ApJ 833, L9.
Loeffler, M.J., et al., 2015. Giant-planet chemistry: ammonium hydrosulfide (NH_4SH), its IR spectra and thermal and radiolytic stabilities. Icarus 258, 181–191.
Loeffler, M.J., et al., 2016. The spectrum of Jupiter's Great Red Spot: the case for ammonium hydrosulfide (NH_4SH). Icarus 271, 265–268.
Loeffler, M.J., et al., 2011. Radiolysis of sulfuric acid, sulfuric acid monohydrate, and sulfuric acid tetrahydrate and its relevance to Europa. Icarus 215, 370–380.
Meyer, B., et al., 1972. The visible spectrum of S_3 and S_4. J. Mol. Spectr. 42, 335–343.
Moore, M.H., et al., 2007a. Ammonia-water ice laboratory studies relevant to outer Solar System surfaces. Icarus 190, 260–273.
Moore, M.H., et al., 2007b. The radiolysis of SO_2 and H_2S in water ice: implications for the icy jovian satellites. Icarus 189, 409–423.
Moses, J.I., et al., 2010. On the abundance of non-cometary HCN on Jupiter. Faraday Discussions 147, 103–136.
Parent, P., et al., 2009. The irradiation of ammonia ice studied by near edge x-ray absorption spectroscopy. J. Chem. Phys. 131, 154308.
Prestel, H., Schindewolf, U., 1987. Identification of the main sulfur nitrogen-compounds in sulfur ammonia solutions. Z. Anorg. Allg. Chem. 551, 21–32.
Raulin, K., et al., 2011. Identification of the EPR signal of S_2^- in green ultramarine pigments. Phys. Chem. Chem. Phys. 13, 9253–9259.
Reuter, D.C., et al., 2007. Jupiter cloud composition, stratification, convection, and wave motion: a view from New Horizons. Science 318, 223–225.
Roman, M.T., et al., 2013. Saturn's cloud structure inferred from Cassini ISS. Icarus 225, 93–110.
Sagan, C., Thompson, W.R., 1984. Production and condensation of organic gases in the atmosphere of Titan. Icarus 59, 133–161.
Schulman, J.H., Compton, W.D., 1962. Color Centers in Solids. Pergamon Press, New York.
Simon-Miller, A.A., et al., 2002. New observational results concerning Jupiter's Great Red Spot. Icarus 158, 249–266.
Simon, A.A., et al., 2015. Spectral comparison and stability of red regions on Jupiter. J. Geophys. Res. 120, 483–494.
Sromovsky, L.A., et al., 2017. A possibly universal red chromophore for modeling color variations on Jupiter. Icarus 291, 232–244.
Sromovsky, L.A., Fry, P.M., 2010a. The source of 3-μm absorption in Jupiter's clouds: reanalysis of ISO observations using new NH_3 absorption models. Icarus 210, 211–229.
Sromovsky, L.A., Fry, P.M., 2010b. The source of widespread 3-μm absorption in Jupiter's clouds: constraints from 2000 Cassini VIMS observations. Icarus 210, 230–257.
Stiles, D.A., et al., 1966. Photolysis of Group VI Hydrides I. Solid H_2S, H_2S_2, and D_2S. Can. J. Chem. 44, 2149–2155.
Strazzulla, G., et al., 2009. The origin of sulfur-bearing species on the surfaces of icy satellites. Adv. Spac. Res. 43, 1442–1445.
Strycker, P.D., et al., 2011. Jovian chromophore characteristics from multispectral HST images. Icarus 215, 552–583.
Weidenschilling, S.J., Lewis, J.S., 1973. Atmospheric and cloud structures of Jovian planets. Icarus 20, 465–476.
West, R.A., et al., 1986. Clouds, aerosols, and photochemistry in the Jovian atmosphere. Icarus 65, 161–217.
Wong, M.H., et al., 2015. Fresh clouds: A parameterized updraft method for calculating cloud densities in one-dimensional models. Icarus 245, 273–281.
Ziegler, J.F., 2010. Stopping and range of ions in matter SRIM2010 (available at www.srim.org).